Materials Today: Proceedings 57 (2022) 1884–1891

Contents lists available at ScienceDirect

Materials Today: Proceedings

journal homepage: www.elsevier.com/locate/matpr

# Free convection heat transfer from a semi-circular cylinder inside a square enclosure: Orientation effects

Jahnavi Mahajan [a], Jaspinder Kaur [a], Roderick Melnik [b,c], Anurag Kumar Tiwari [a,*]

[a] Department of Chemical Engineering, National Institute of Technology, Jalandhar 144011, Punjab, India
[b] Wilfrid Laurier University, 75 University Avenue West, Waterloo, ON N2L 3C5, Canada
[c] BCAM Basque Center for Applied Mathematics, Mazarredo Zumarkalea, 14, 48009 Bilbo, Bizkaia, Spain

ARTICLE INFO

*Article history:*
Available online 24 January 2022

*Keywords:*
Free convection
Power-law fluid
Rayleigh number
Nusselt number

ABSTRACT

The numerical investigation has been carried out for the buoyancy driven flow (free convection) from a cylinder of semi-circular cross-section at three orientation angles (i.e., $\varphi = 0^{\circ}, 45^{\circ}$ and$90^{\circ}$) to stagnant power-law fluids inside a square cavity. The coupled governing equations were solved for the given range of the pertinent dimensionless parameters of Rayleigh number ($10^2 \leqslant Ra \leqslant 10^5$), Prandtl number ($10 \leqslant Pr \leqslant 100$), and power-law index ($0.3 \leqslant n \leqslant 1.8$). At different orientation angles of the semi-circular cylinders, the numerical results were visualized in terms of velocity and temperature profiles near the cylinder and, gross engineering parameters (e.g., average Nusselt numbers). If all other factors are equal, the rate of heat transfers from a semi-circular cylinder at $\varphi = 90^{\circ}$ is higher than for the other orientations. The rate of heat transfer can also be increased by increasing the value of Ra and decreasing the value of Pr. In the power-law fluids, the heat transfer rate is always higher in shear-thinning fluids under the same condition. In the end, the average Nusselt number for different orientation angles of the cylinder has been correlated by simple expression.


## 1. Introduction

Over the last few years, free convection inside the cavity has been an important research field for fundamental and practical use. Some practical applications are melting and heating polymeric pellets, heat exchangers, nuclear and chemical reactors, energy storage devices, and cooling electronic components. The coupled governing equations via temperature-dependent buoyancy term are solved simultaneously, affecting the overall heat transfer process to varying extents. Moreover, due to the coupled governing equations, this problem is admitted the enormous challenges in computational simulation.

The buoyancy-driven heat transfer from the cylinder of various shapes inside the enclosure has another well-known study for practical consideration. Most of the available literature [1] investigated heat transfer in free convection mode from a circular cylinder inside the enclosure. First, Roychowdhury et al. [2] studied the free convection from a circular cylinder inside the square enclosure. The systematic investigation has highlighted the effect of different thermal conditions on heat transfer. Next, Larson et al. [3] carried out free convection from a circular cylinder inside the rectangular cavity through the numerical simulation and experimentally. They validated the numerical results of the temperature field experimentally and found good agreement. Next, Oosthuizen with co-workers [4] investigated the same problem with different boundary conditions on the cavity walls. Cesini et al. [5] studied the free convection from the circular cylinder placed at the centre of the rectangular enclosure filled with Newtonian fluids. Over the range of conditions, they found that the effect of Rayleigh number and geometry of the cavity significantly affects heat transfer rate. Kim et al. [6] studied the natural convection at a high Rayleigh number. Here, the heat transfer rate is affected by the location of the cylinder inside the enclosure/cavity. Subsequently, Lee et al. [7] studied the diagonal position of the circular cylinder inside the square enclosure, and it is found the appreciable effect on heat transfer. Similarly, Hussain and Hussein [8] looked at free convection from the circular cylinder at constant wall flux boundary conditions inside the square enclosure. As a result, the average Nusselt number is strongly affected by cylinder locations. Finally, in contrast to the circular cylinder, De and Dalal [9] studied the heat transfer in the laminar free convection regime

* Corresponding author.
*E-mail address:* tiwaria@nitj.ac.in (A.K. Tiwari).

https://doi.org/10.1016/j.matpr.2022.01.207

for a tiled square cylinder confined by a square enclosure. The given range of Rayleigh numbers found a significant influence on heat transfer when the heated square cylinder changes vertically. In the case of non-Newtonian fluids, Sairamu and Chhabra [10] investigated the effect of power-law fluids over the tilted square cylinder in a square enclosure. In the results, the heat transfer rate is affected by the cylinders' location (off-centre positions) inside the enclosure.

In present the problem, the governing equation has been solved computationally for a heated semi-circular cylinder with the surrounding power-law fluid inside a long square enclosure, with three orientation angles of the cylinder ($0^\circ \leqslant \varphi \leqslant 90^\circ$). The numerical results explored herein over parameters: $10^2 \leqslant Ra \leqslant 10^5$, $10 \leqslant Pr \leqslant 100$, $0.3 \leqslant n \leqslant 1.8$ and $d/L = 0.25$. Furthermore, walls of the square enclosure are treated as cold walls whereas the surfaces of the semi-circular cylinder are maintained by the isothermal boundary condition with the higher temperature on the surface than that of the enclosure walls. This model configuration understands the overall heat transfer of a tubular heat exchanger in which the semi-circular tubes are arranged in various orientation angles of the cylinder.

## 2. Mathematical model

Two- dimensional semi-circular cylinder of diameter $d$ is situated at the centre of the square cavity of side length $L$ (Fig. 1). The space between them is filled with power-law fluid and the surface of the cylinder is maintained at constant wall temperature (CWT). Under the consideration of small temperature difference, the thermo-physical properties of the fluid ($C_p$, $k$, $m$, and $n$) including the fluid density (except $y$-component of momentum equation) is assumed to be temperature-independent. The density term in y-component is approximated by Boussinesq approximation, (e.g.,$\rho = \rho_\infty(1 - \beta(T - T_\infty))$).

In the incompressible fluid, the extra stress tensor $\tau_{ij}$ is defined as follows, (Bird et al. [11]),

$$\tau_{ij} = 2\eta\varepsilon_{ij}, \text{where } (i,\ j) = (x,\ y). \tag{1}$$

The rate of deformation tensor is denoted as $\varepsilon_{ij}$ and scalar viscosity $\eta$ in the Eq.1 is related to each other,

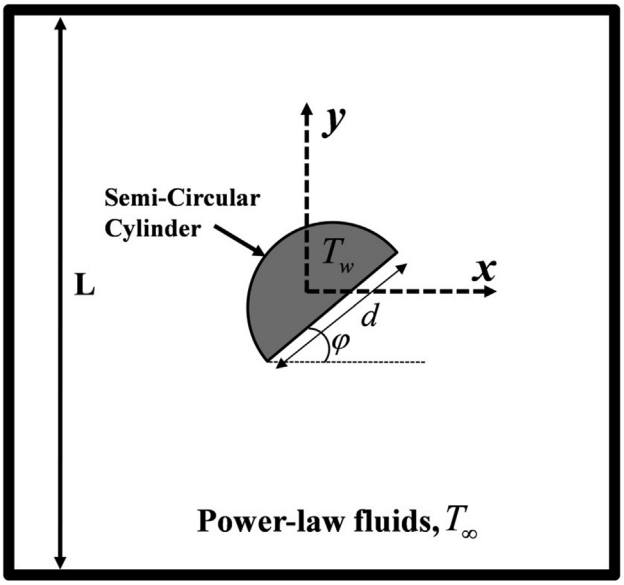


**Fig. 1.** Schematic representation of free convection heat transfer insides the square enclosure.

$$\eta = m(I_2/2)^{(n-1)/2}, \tag{2}$$

where $I_2$ is the second invariant of the shear rate (Bird *et al.* [11]). In Eq. (2), $m$ and $n$ are indicated the consistency and power-law index respectively. For power-law fluids, $n = 1$(Newtonian fluids),$n > 1$ (shear-thickening fluids) and $n < 1$ (shear-thinning fluids). In the given framework of assumptions as mentioned above, the coupled governing equations in their dimensionless forms are written as follows:

Continuity Equation:

$$\frac{\partial u_i}{\partial x_i} = 0 \tag{3}$$

Momentum Equation:

$$u_j\frac{\partial u_i}{\partial x_j} = -\frac{\partial p}{\partial x_i} + \delta_{i2}RaPr\theta + \frac{\partial \tau_{ij}}{\partial x_j} \tag{4}$$

Energy Equation:

$$u_j\frac{\partial u_i}{\partial x_j} = \frac{\partial^2\theta}{\partial x_j\partial x_i} \tag{5}$$

In the above governing Eqs. (3)-(5), the spatial coordinate $x_i$, velocity components $u_i$, pressure, $p$, stress component, $\tau_{ij}$ and temperature are scaled as follows,

$$x_i = \frac{x_i^1}{L}, u_i = \frac{u_i^1}{u_{ch}}, p = \frac{p^1}{\rho u_{ch}}, p = \frac{\tau_{ij}^1}{\rho\alpha u_{ch}/L},$$
$$\theta = \frac{(T - T_\infty)}{(T_w - T_\infty)}, \text{and} \quad u_{ch} = \alpha/L, \text{where } \alpha = k/\rho C_p \tag{6}$$

At this juncture, it is thus appropriate to introduce some of their non-dimensional parameter definitions used in Eqs. (3)-(5) as follows,

$$Ra = \frac{g\beta\Delta TL^{2n-1}}{\alpha^n(m/\rho)}, Pr = \left(\frac{m}{\rho}\right)\alpha^{n-2}L^{2-2n} \tag{7}$$

where $\beta$ and $g$ is thermal expansion coefficient and acceleration due to gravity, respectively. The problem statement is completed by specifying the realistic boundary conditions in the computation domain. At the surface of the semi-circular cylinder and walls of the square enclosure, no-slip boundary condition ($u_x = 0$ and $u_y = 0$) is prescribed. The cold enclosure walls are maintained at $\theta = 0$ whereas the hot semi-circular cylinder is maintained at $\theta = 1$.

The average Nusselt number for natural convection of power-law fluids in square enclosure can be represented as functional relationship, $Nu_{avg} = f(Ra, Pr, n, \varphi)$. Generally, the local Nusselt number varies from point to point on the surface of the cylinder and it is defined as:

$$Nu = \frac{hd}{k} = -\frac{\partial\theta}{\partial n_s} \tag{8}$$

where $d$ is the diameter of the cylinder, $n_s$ is the outward drawn unit normal vector on the surface of the semi-circular cylinder. The surface averaged Nusselt number $Nu_{avg}$ is obtained simply by integrating the local values over the surface of the semi-circular cylinder as:

$$Nu_{avg} = \frac{1}{S}\int NudS \tag{9}$$

Dimensional considerations suggest Nusselt number to be influenced by the dimensionless groups, namely, Rayleigh number ($Ra$), Prandtl number ($Pr$), power-law index ($n$), and orientation angle of the semi-circular cylinder ($\varphi$). In the present work, the geometry of the square enclosed $d/L = 0.25$ is fixed whereas the remaining parameter is varied over the given ranges to depict their effect on the free convection heat transfer.

## 3. Results and discussion

### 3.1. Numerical methodology

The coupled governing equations (Eqs. (3)–(5)) and boundary conditions are solved with finite element based software (COMSOL Multiphysics). The computational domain was meshed using a fine mesh with triangular elements near the cylinder and wall of the enclosure to capture sharp velocity and temperature gradient. Here, we have investigated the numerical results in the laminar steady-state regime. Under the 2-D fluid flow, the heat transfer module is used to solve the governing equations. The buoyancy induced term is included by using a volume force term. The relative convergence criterion $10^{-5}$ was used for the fluid flow and heat transfer equation [12].

Here, the computational domain of the problem is fixed ($d/L = 0.25$). The minimum grid sizes are required for accurate numerical results. Therefore, three different grid size (*i.e.*, G1 (N = 46000), G2 (N = 55000), G3 (N = 65000)) is used for each orientation angle $\varphi$ which is used in our grid test results. The grid test results were performed at the maximum values of the Rayleigh ($Ra = 10^5$), Prandtl numbers ($Pr = 100$) and power-law index ($n = 0.3$). The influence of grid size is indicated in term of the local Nusselt number on the surface of the semi-circular cylinder for three orientation angle (e.g.,$\varphi = 0^\circ, 45^\circ$ and$90^\circ$), as shown in Fig. 2. By changing the grid size from G2 to G3, the change in results is <2% and thus, G2 was found to be optimum grid size for the present investigation. The non-uniform grid G2 with minimum size ($\delta = 0.0125$) on the surface of the cylinder is used for present studies. The numerical results reported in this study have been calculated with 55,000 elements with minimum grid size on the surface of the cylinder $\delta = 0.0125$ and fixed computational domain ($d/L = 0.25$).

### 3.2. Validation of results

It is important to demonstrate the general validity of the numerical solution methodology used here. This objective is achieved here by validating the well-known reliable results for the horizontal circular cylinder in the circular annulus. The numerical results are presented in terms of average Nusselt number with literature results at different values of Rayleigh number (Fig. 3). The present numerical values differ from that of Raithby and Hollands [13] by ~ 2–3%, the corresponding deviations are of the order of ~ 3–4% from that of Grigull and Hauf [14].

### 3.3. Streamline and isotherm contours

In the streamline profiles Fig. 4, at low values of the Rayleigh number, advection is seen to be weak (e.g., small

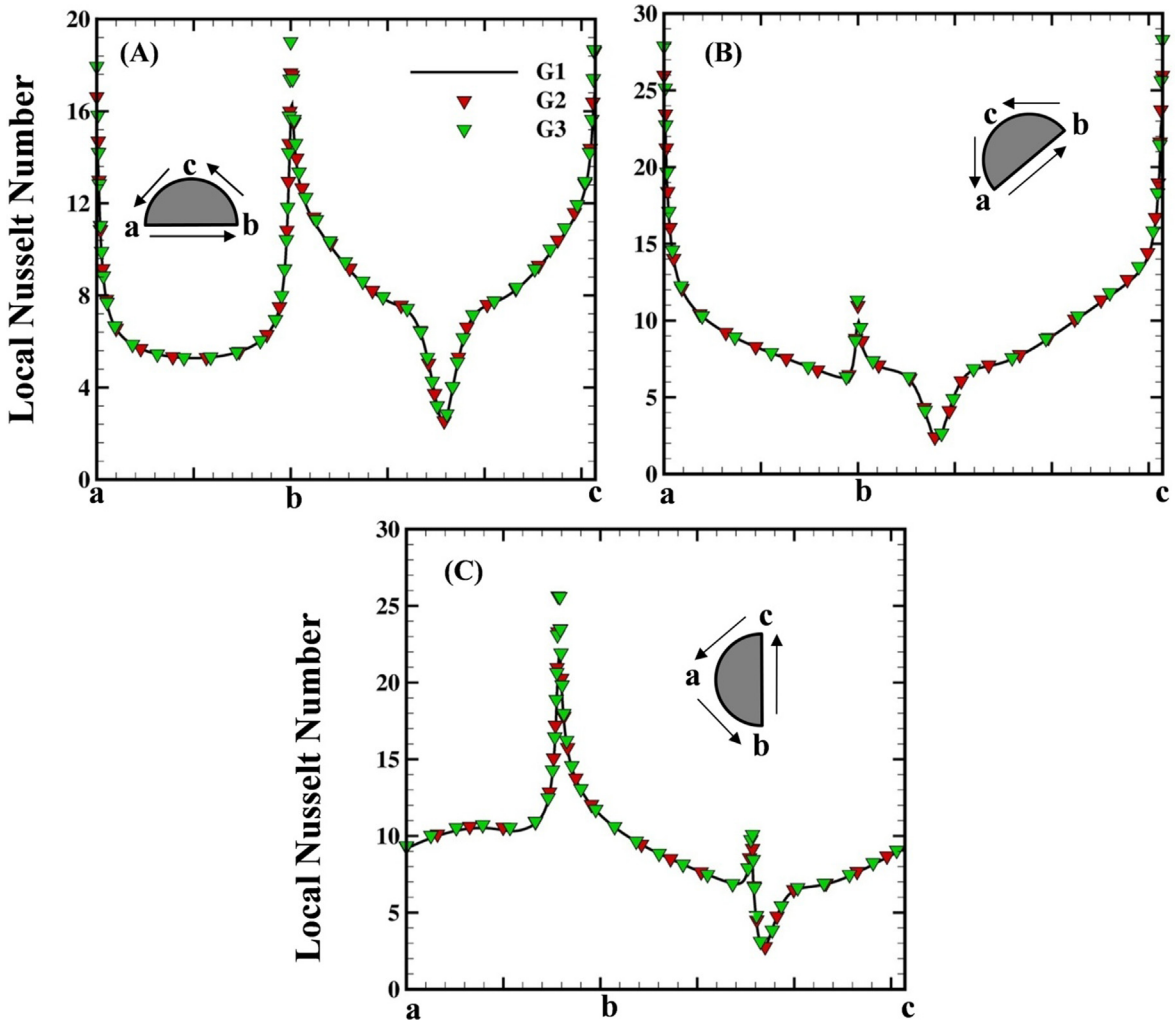


**Fig. 2.** Effect of grid size on the distribution of the local Nusselt number along the surface of the semi-circular cylinder for (A) $\varphi = 0^\circ$,(B) $\varphi = 45^\circ$ and (C)$\varphi = 90^\circ$.

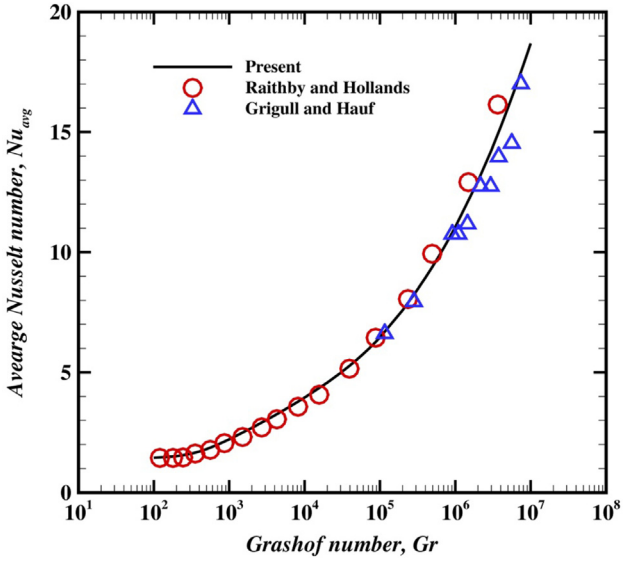


**Fig. 3.** Comparison of the present average Nusselt number (solid line) with the predictions of Raithby and Hollands [13] and Grigull and Hauf [14] in the air for configuration $D/d = 4$, respectively.

values of $\psi$), and heat transfer occurred only by conduction mode. Due to weak buoyancy-induced flow, one can predict the formation of the two recirculation regions (oriented in the opposite direction) formed above the semi-circular cylinders. The hot fluids rise above the semi-circular cylinder (e.g. temperature dependent density of the fluids) and flow back towards the cold region inside the enclosure with a small fraction of it descending along the side walls. This, in turn, generated recirculation patterns, above the beneath of the cylinder. In the presence of weak advection at $Ra = 1000$ or 100, the effects of power-law index and orientation angles of the cylinder are almost negligible under these conditions. However, as the Rayleigh number is increased to $Ra = 10^5$, the buoyancy-induced flow current becomes stronger which augmented values of $\psi$ (e.g., crowing of streamline profiles near the cylinder). The extent of fluid recirculation (qualitative manner) is seen to be maximum in shear-thinning fluids ($n < 1$) which progressively decreases as the fluid behaviour changes Newtonian ($n = 1$) and shear-thickening behaviour ($n > 1$). This difference can be seen due to the lowering of the effective fluid viscosity at $n < 1$ and the corresponding increase in the fluid viscosity for a shear-thickening fluid at $n > 1.8$. Next, an important parameter is the orientation of the cylinder inside the enclosure, crowing of streamline profiles is also increases with increasing the orientation angle of the cylinder.

In Fig. 5, at low $Ra = 10^3$, isotherm contours near the surface of the cylinder are followed more or less similar to the shape of the cylinder which indicated the low convection current and heat transfer dominated by conduction mode. At the higher value of $Ra = 10^5$, the buoyancy-induced current becomes stronger and heat transfer dominated by convection mode as shown in Fig. 5. At higher value of Ra, the fluids above the cylinder are mobilized and gradually thinning the thermal boundary layer near the cylinder. As a result, pairs of two recirculation zone are observed at the higher value of $Ra = 10^5$, irrespective of power-law index, Pr and orientation angle (see Fig. 4). For fixed values of Rayleigh number and Prandalt number, the thermal boundary layer is seen to be thinner in shear-thinning fluids ($n < 1$) than that in Newtonian ($n = 1$) and shear-thickening ($n > 1.0$) fluids irrespective of orientation angle. On the other hand, it is also predicted the effect of the orientation angle of the cylinder inside the enclosure. The bending and distortion of isotherm contours near the cylinder increase with orientation angle, thereby thin boundary layer formation from $\varphi = 0°$ to 90° which promoted heat transfer from the cylinder. Thus, the heat transfer rate is higher for the semi-circular cylinder at $\varphi = 90°$ as compared to others.

### 3.4. Variation of average Nusselt number

Fig. 6 represented the variation of the average Nusselt number with power-law index ($n$) at different orientation angles of the semi-circular cylinder at $Ra = 10^3$ and $Ra = 10^5$. The variation of $Nu_{avg}$ with power-law index increases with increasing value of orientation angle (e.g., $\varphi = 0^\circ$ to $\varphi = 90^\circ$) at a fixed value of $Ra$ and $Pr$. It is clearly observed that at a low value of Ra (e.g., $Gr = 10^2$ and $Pr = 10$ or $Ra = 10^3$), the values of $Nu_{avg}$ are almost constant under the conduction dominant region. As the values of $Nu_{avg}$ increase with increasing value of $Ra$ (e.g., $Gr = 10^4$, $Pr = 10$ and $Gr = 10^3$, $Pr = 100$ or $Ra = 10^5$) which is indicated by the strong buoyancy induced convection current with varying levels of enhancement in $Nu_{avg}$ for shear-tinning fluids and shear-thickening fluids. This effect is consistent with the scaling argument, $Nu_{avg} \sim (Ra^{2-n}Pr^{-n})^{1/2(n+1)} f(Ra, Pr, n)$ which is suggested by Turan et al. [15]. Due to varying fluid viscosity of power-law fluids, Shear-thickening fluids (n > 1) is restricted growth of the wake and thermal plume is due to the rapid increase in the fluid viscosity which is decreasing levels of fluid shearing layers. Such an increase in effective fluid viscosity, in turn, lowers the rate of heat transfer under these conditions. The value of $Nu_{avg}$ decreases with the increasing value of $Pr$ for shear-thinning fluids ($n = 0.3$), the value of $Nu_{avg}$ remains constant with increasing value of $Pr$ for Newtonian fluids ($n = 1$) and the variation of $Nu_{avg}$ increases with the increasing value of $Pr$ for shear thickening fluids ($n = 1.8$). These trends are consisten for each orientation angle at $Ra = 10^3$ and $Ra = 10^5$. The thermal boundary layer ($\delta_{th} \sim 1/Nu_{avg}$) is expected to be thinner as compared to the hydrodynamic boundary layer for increasing value of $Pr$ and this effect is higher in the lower value of power-law index. The variation of $Pr$ on $Nu_{avg}$ is more pronounced at $\varphi = 90^\circ$ as compared to other orientation angles.

The local Nusselt number on the surface of the cylinder, which indicates the outward normal temperature distribution on the surface of the cylinder, can be used to illustrate the detailed variation of heat transfer (e.g., Eq. (8)). The variation of the local Nusselt number on the surface of the cylinder at different orientation angles $\varphi$ is shown in Fig. 7 over the range of parameters ($Ra$, $Pr$, and $n$). At the fixed value of $Ra$, $n$, and $Pr$, the variation of local Nusselt number increases with orientation angle, as can be seen ($0^\circ \leqslant \varphi \leqslant 90^\circ$). This is due to thinning of the thermal boundary layer near the surface of the semi-circular cylinder inside the enclosure, as shown in the streamline and isotherm contours for shear-thinning fluids (n < 1), Newtonian fluids (n = 1), and shear-thickening fluids (n > 1), respectively. It can be seen in Fig. 4-5, the magnitude of the isotherm contours more distorted and stream function increases with increasing the orientation from $\varphi = 0^\circ$ to $\varphi = 90^\circ$. This effect indicated the thickness of the thermal boundary layer that depends on the frontal contact area of the cylinder. When the cylinder is at an angle, $\varphi = 90^\circ$, the less frontal contact area of the cylinder in the direction of buoyancy flow decreases the boundary layer as compared to the other orientation angle and that is directly increasing $Nu_{avg}$. Thus, the value $Nu_{avg}$ increases with orientation angle from $\varphi = 0^\circ$ to $\varphi = 90^\circ$

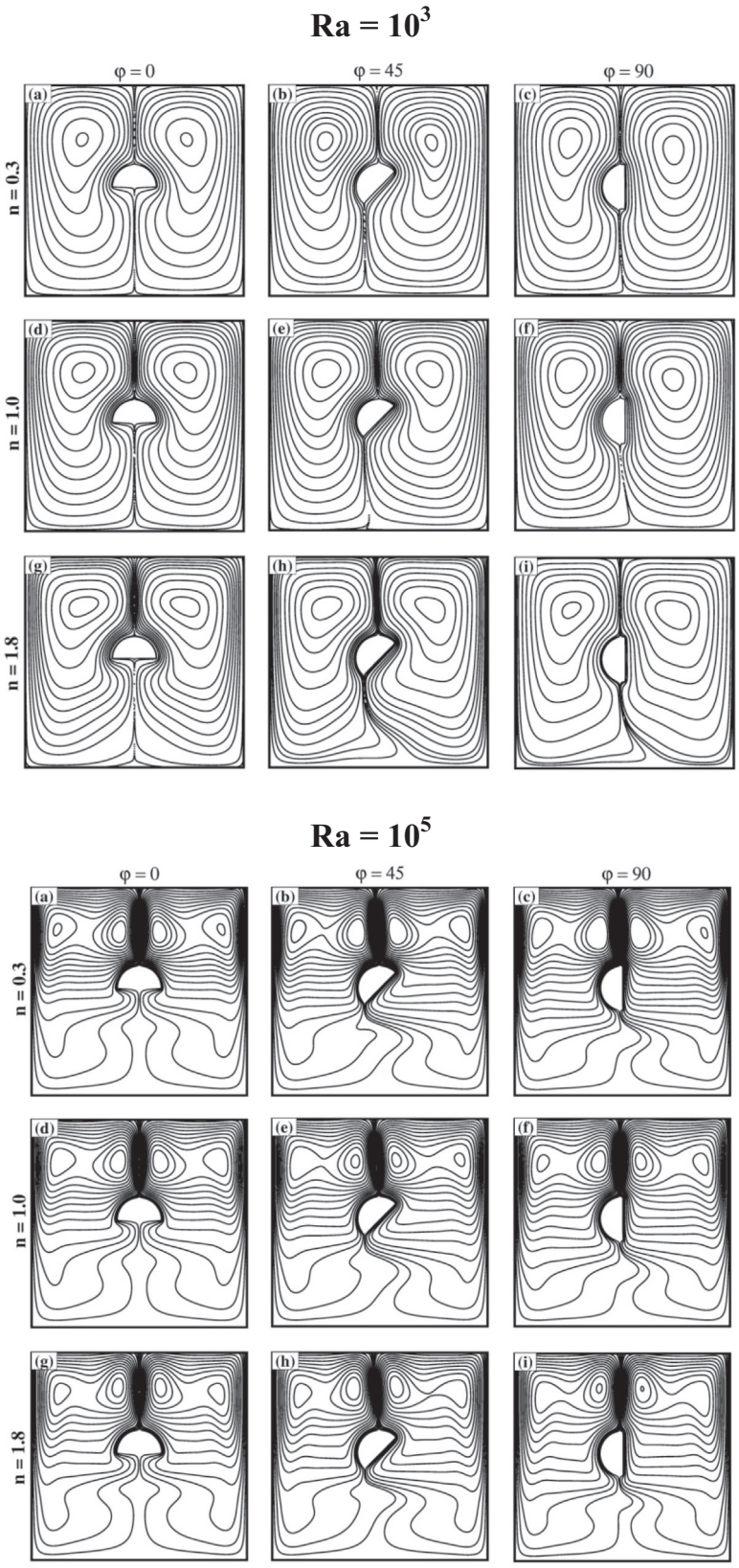


**Fig. 4.** Variation of streamline profiles for different orientation angles ($\varphi = 0^{\circ}, 45^{\circ}, 90^{\circ}$) in the case of shear-thinning ($n = 0.3$), Newtonian ($n = 1.0$) and shear-thickening ($n = 1.8$) fluids at $Ra = 10^5$ and $Pr = 100$.

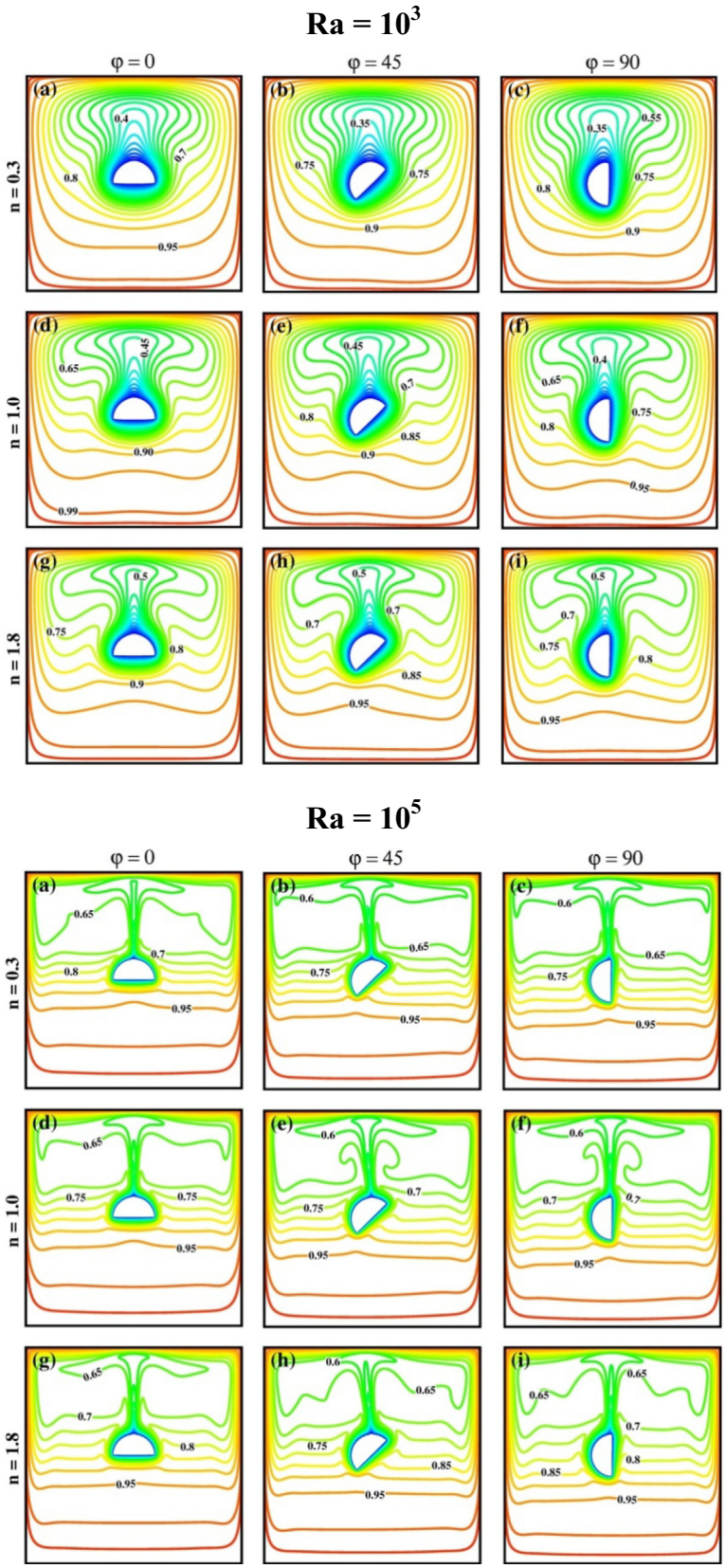


**Fig 5.** Variation of non-dimensional temperature profile for different orientation angle ($\varphi = 0^{\circ}, 45^{\circ}, 90^{\circ}$) in the case of shear-thinning ($n$ = 0.3), Newtonian ($n$ = 1.0) and shear-thickening ($n$ = 1.8) fluids at $Ra = 10^5$ and $Pr$ = 100.

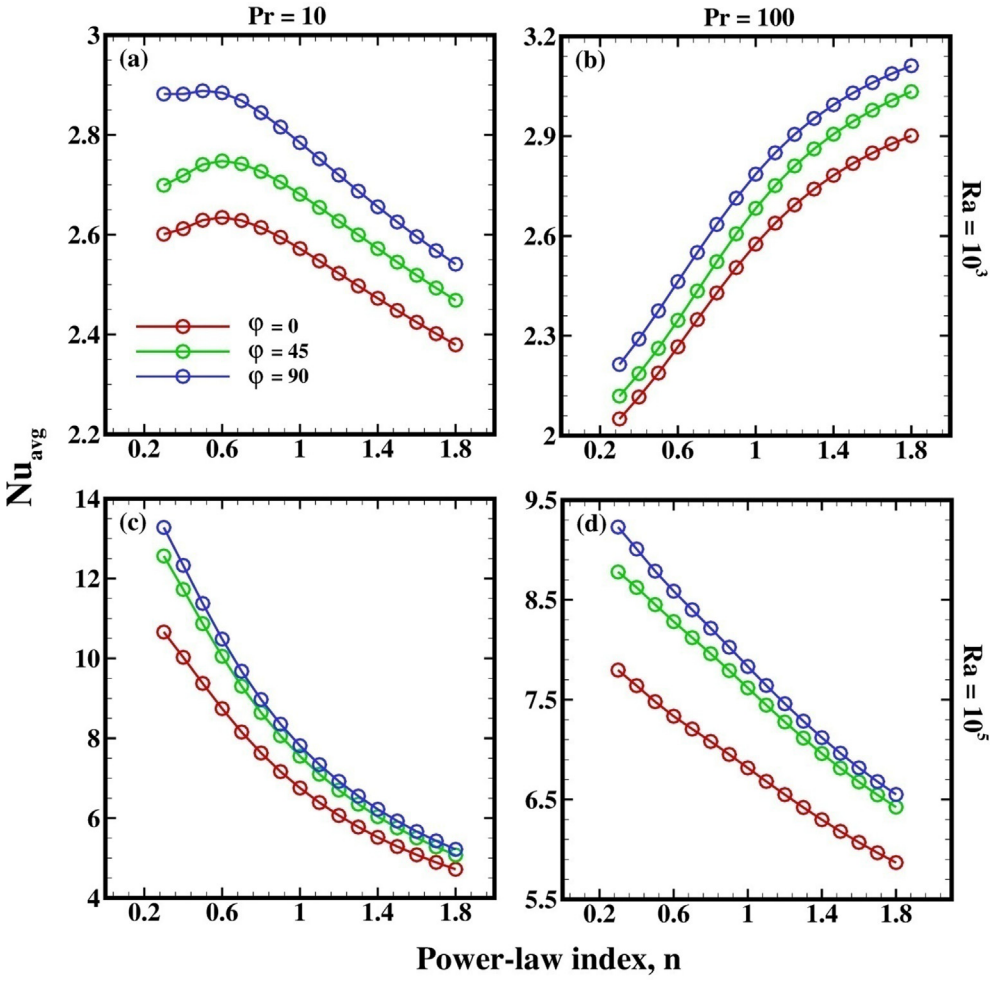


**Fig. 6.** Variation of $Nu_{avg}$ with power-law index at different values of Ra, Pr and φ.

### 3.5. Correlation for average Nusselt number

From the engineering application point of view, it is needed to develop a predictive correlation of the average value of the Nusselt number for each orientation angle of the cylinder. The following expression can adequately approximate the present numerical results,

$$\text{For } \varphi = 0^\circ : Nu_{avg} = Nu_\infty + 0.0097Ra^{1.078\left(\frac{n}{n+1}\right)}\left(\frac{Pr}{1.292+Pr}\right)^{-0.8092}\left(\frac{3n+1}{4n}\right)^{-1.88} \quad (10)$$

$$\text{For } \varphi = 45^\circ : Nu_{avg} = Nu_\infty + 0.0058Ra^{1.186\left(\frac{n}{n+1}\right)}\left(\frac{Pr}{0.680+Pr}\right)^{-1.881}\left(\frac{3n+1}{4n}\right)^{-2.083} \quad (11)$$

$$\text{For}\varphi = 90^\circ = Nu_{avg} = Nu_\infty + 0.0012Ra^{1.452\left(\frac{n}{n+1}\right)}\left(\frac{Pr}{1.477+Pr}\right)^{-1.388}\left(\frac{3n+1}{4n}\right)^{-2.524} \quad (12)$$

Where $Nu_{avg} \to Nu_\infty$ indicates the conduction limit at low values of the Rayleigh number. The average and maximum deviations are ∼ 11.28% and ∼ 47.56% for Eq.10, ∼12.74% and ∼ 49.17% for Eq.11 and ∼ 12.74% and ∼ 49.17% for Eq.12 respectively, over the range of the condition as, $10^2 \le Ra \le 10^5$, $10 \le Pr \le 100$and$0.3 \le n \le 1.8$. Only a few data points show the deviation of >13% and most of the data are related to conduction dominated region. Finally, it is worthwhile to add the limiting case for Newtonian behaviour ($n = 1$), all the equations roughly yield, $Nu_{avg} \propto Ra^{1/4}$, which is consistent with the literature.

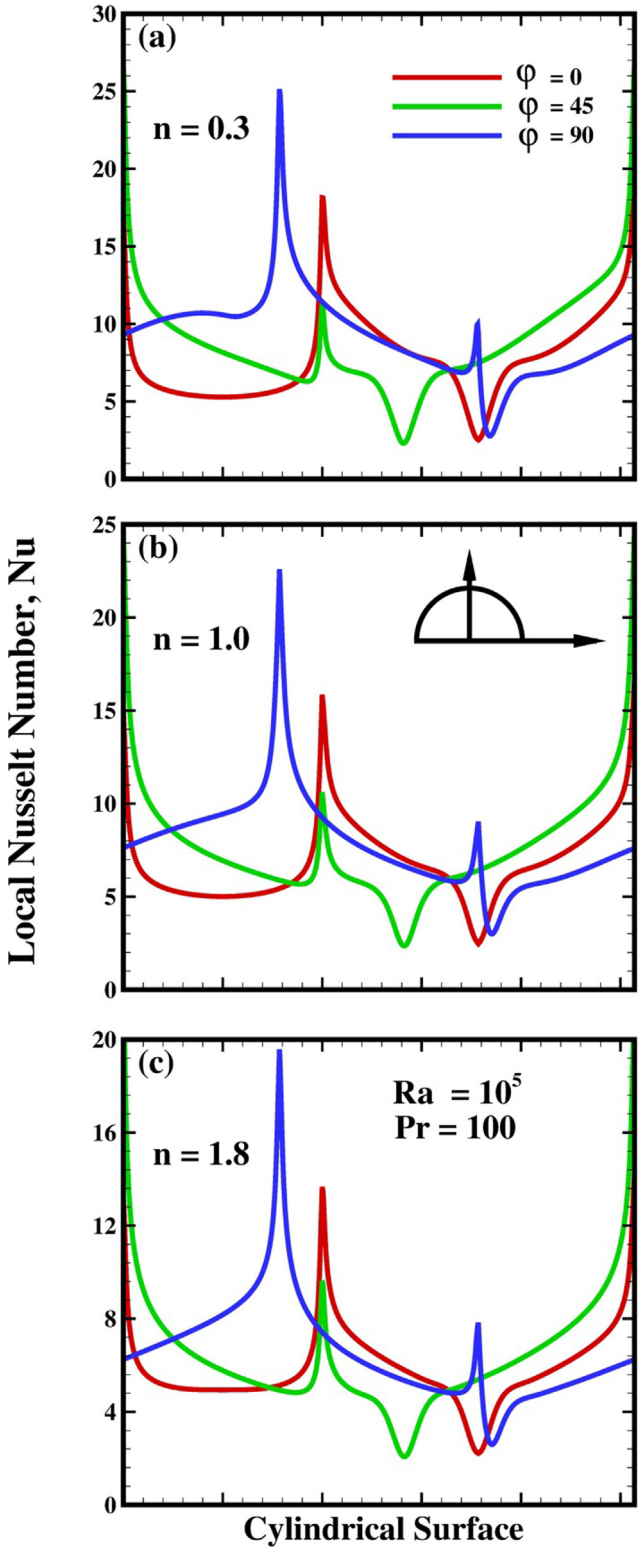


**Fig. 7.** Variation of the local Nusselt number on the surface of the cylinder.

## 4. Conclusion

In this present work, heat transfer from a semi-circular cylinder to power-law fluids filled in a square enclosure has been investigated. This work elucidates the influences of orientation ($0^{\circ} \le \varphi \le 90^{\circ}$) of the semi-circular cylinder over the range of dimensionless parameters, $10^2 \le Ra \le 10^5$, $10 \le Pr \le 100$, and $0.3 \le n \le 1.8$ considered here. It has been observed that the average Nusselt number ($Nu_{avg}$) shows a positive function with both Rayleigh and Prandtl numbers due to the increasing strength of the convective transport. The effect of the orientation angle of the semi-circular cylinder is exerted an appreciable influence on $Nu_{avg}$. The effect of the power-law index on the average Nusselt number is found to be entwined due to decreased effective viscosity. It is possible to realize some enhancement in the rate of heat transfer at semi-circular cylinder at $\varphi = 90^{\circ}$ under appropriate conditions, namely, at high values of the Rayleigh and Prandtl numbers. The present average Nusselt number data is correlated in simple expression to estimate the average Nusselt number for new engineering applications.

## Declaration of Competing Interest

The authors declare that they have no known competing financial interests or personal relationships that could have appeared to influence the work reported in this paper.

## Acknowledgements

The authors are grateful to Dr. Neelkanth Nirmalkar, Assistant Professor, Department of Chemical engineering, Indian Institute of Technology Ropar India, for his continued support and for proving us with the computational facility.

## References

[1] R.P. Chhabra, J.F. Richardson, Non-Newtonian Flow and Applied Rheology: Engineering Applications, second edition., Butterworth-Heinemann, Oxford, 2008.
[2] D.G. Roychowdhury, S.K. Das, T. Sundararajan, Numerical simulation of natural convective heat transfer and fluid flow around a heated cylinder inside an enclosure, Heat Mass Transfer 38 (7-8) (2002) 565–576, https://doi.org/10.1007/s002310100210.
[3] D.W. Larson, D.K. Gartling, W.P. Schimmel, Natural convection studies in nuclear spent-fuel shipping casks: computation and experiment, J. Energy 2 (3) (1978) 147–154, https://doi.org/10.2514/3.62373.
[4] P.H. Oosthuizen, Z. Xu, Heat Transfer Processes, in: Proc. 29th National Heat Transfer Conference, 1993; 252;83–89.
[5] G. Cesini, M. Paroncini, G. Cortella, M. Manzan, Natural convection from a horizontal cylinder in a rectangular cavity, Int. J. Heat Mass Transfer 42 (10) (1999) 1801–1811, https://doi.org/10.1016/S0017-9310(98)00266-X.
[6] B.S. Kim, D.S. Lee, M.Y. Ha, H.S. Yoon, A numerical study of natural convection in a square enclosure with a circular cylinder at different vertical locations, Int. J. Heat Mass Transfer 51 (7-8) (2008) 1888–1906, https://doi.org/10.1016/j.ijheatmasstransfer.2007.06.033.
[7] J.M. Lee, M.Y. Ha, H.S. Yoon, Natural convection in a square enclosure with a circular cylinder at different horizontal and diagonal locations, Int. J. Heat Mass Transfer 53 (25-26) (2010) 5905–5919, https://doi.org/10.1016/j.ijheatmasstransfer.2010.07.043.
[8] S.H. Hussain, A.K. Hussein, Numerical investigation of natural convection phenomena in a uniformly heated circular cylinder immersed in square enclosure filled with air at different vertical locations, Int. Commun. Heat Mass Transfer 37 (8) (2010) 1115–1126, https://doi.org/10.1016/j.icheatmasstransfer.2010.05.016.
[9] A. Kumar De, A. Dalal, A numerical study of natural convection around a square, horizontal, heated cylinder placed in an enclosure, Int. J. Heat Mass Transfer 49 (23-24) (2006) 4608–4623, https://doi.org/10.1016/j.ijheatmasstransfer.2006.04.020.
[10] M. Sairamu, R.P. Chhabra, Natural convection in power-law fluids from a tilted square in an enclosure, Int. J. Heat Mass Transfer 56 (1-2) (2013) 319–339.
[11] R.B. Bird, W.E. Stewart, E.N. Lightfoot, Transport Phenomena, Wiley, 2006.
[12] A.K. Tiwari, R.P. Chhabra, Laminar natural convection in power-law liquids from a heated semi-circular cylinder with its flat side oriented downward, Int. J. Heat Mass Transfer 58 (1-2) (2013) 553–567, https://doi.org/10.1016/j.ijheatmasstransfer.2012.11.051.
[13] G.D. Raithby, K.G.T. Hollands, T.E. Unny, Analysis of heat transfer by natural convection across vertical fluid layers, J. Heat Transfer 99 (2) (1977) 287–293, https://doi.org/10.1115/1.3450683.
[14] U. Grigull, W. Hauf, Proceedings of the 3rd International Heat Transfer Conference 1966; 2; 182.
[15] O. Turan, A. Sachdeva, N. Chakraborty, R.J. Poole, Laminar natural convection of power-law fluids in a square enclosure with differentially heated side walls subjected to constant temperatures, J. Nonnewton. Fluid Mech. 166 (17-18) (2011) 1049–1063.